Available online at www.sciencedirect.com
SCIENCE DIRECT®
Theoretical and Applied Fracture Mechanics 39 (2003) 73–88
theoretical and applied fracture mechanics
www.elsevier.com/locate/tafmec

Fractal characteristics of rocks fractured under tension

T. Babadagli [a,*], K. Develi [b,1]

[a] Department of Petroleum and Mineral Research Engineering, College of Engineering, Sultan Qaboos University, P.O. BOX 33, Al-Khod, Muscat 123, Oman
[b] Department of Geological Engineering, Istanbul Technical University, Maslak, Istanbul, Turkey

Abstract

Fractal geometry can be useful for explaining the fracture behavior and rock properties. The fractal properties of rock fracture surface developed under tension were examined. Seven different rock samples were selected for the tests. An automated surface scanning device was used to map the fractured surfaces. Variogram analysis (VA) (for 1D self-affine sets) and power spectral density (PSD) measurement (for 2D self-affine sets) were applied to calculate the fractal dimension. On a comparative basis, there exists a trend between the fractal dimension and loading rate. The profiles in the loading direction yield higher fractal dimensions indicating the anisotropic feature of fractal. The fractal dimensions obtained by PSD and VA display a relationship for grain size and porosity. Higher porosity samples give different fractal dimensions for upper and lower fractures surfaces.

Keywords: Fractal dimension; Variogram analysis; Power spectral density; Tensile fractures; Synthetic rock fracture surfaces; Porosity; Gryain size

1. Introduction

Substantial work has been done on data acquisition of fractals for rock surfaces ever since the fracture surfaces have been shown to represent fractal characteristic [1–3]. Considerable work, however, is needed to show whether the fractal characteristics of the surface roughness is in any way related to the hydraulic and mechanical behavior of fracture. Such a relation, when established, could be useful for quantifying fracture surface data.

Correlation of the surface roughness to the fracture parameters can serve a useful purpose in modeling. To this end, crack propagation has been examined [4] by identifying the relevant fracture parameters. The peak shear stress was correlated to the fractal dimension [5] of the fracture surfaces. Similar results with artificial joint samples were reported in [6,7]. Proposed in [8] are correlations among six roughness parameters including the fractal dimension of surface subjected to shear stress. A new peak shear strength criterion was introduced [9] for anisotropic peak shear strength

* Corresponding author. Now with the University of Alberta, Dept. of Civil and Env. Eng. School of Mining and Petroleum. Tel.: +1-780-492-96-26; fax: +1-780-492-02-49.
E-mail address: tayfun@ualberta.ca (T. Babadagli).
[1] Present address: General Directorate of Rural Services, Gaziantep Province Directorate, Gaziantep, Turkey.

0167-8442/03/$ - see front matter
PII: S0167-8442(02)00139-8

of rock joints. They correlated the peak shear strength to effective normal stress, joint compressive strength, basic friction angle and stationary roughness parameter.

All of the above studies involve correlating the fractal dimension of fracture surface to the shear stress before and after the test. This study aims to investigate the relationship between the initial rock and fracture conditions involving the rock properties and loading rate, and surface roughness yielding after fracture. This is relevant to hydraulic fracturing of oil, gas or geothermal wells. The information can be useful to earthquake studies.

In similar studies, fracture data have been obtained for the shear and tensile tests. Computed are the fractal dimension of fracture profiles in different directions using the variogram method [10]. They related the fractals to the roughness and asperities. The same method was applied in [11]. Poor correlation was found between the fractal dimension and the shear stiffness of rock joints. The conclusion was that the fractals were not sufficient to quantify the surface roughness for predicting the mechanical behavior of rock joints. It was indicated [12] that the multifractal spectrum of fracture surfaces provides more information on the fracturing mechanism and the distribution of asperity concentration on the surface after applying divider method to measure the fractal profiles in different directions. Considerable changes of fractals were observed for tensile and shear fracture. 2D variogram analysis (VA) was made [13] to the data acquired from the morphology of two mortar replicas of granite and schist samples. They applied three different shear stresses. In addition to fractal dimension, parameters were defined to characterize joint surface specific roughness and degradation of sheared joint surface. These parameters were correlated to applied normal stress. The roughness of fracture surface was correlated [14] to the petrophysical properties of cement paste and mortar. Studied in [15] is the effect of loading rate on the fractal dimension of the fracture surfaces in gabbro. It was found that the fractal dimension of the static fracture surfaces of gabbro were approximately constant. But, the fractal dimensions of dynamic fracture surfaces increased with increasing loading rate.

In what follows, attention is focused on the loading stress during indirect tensional tests (Brazilian) and rock properties. The data are correlated to the fractal properties of the surface roughness.

2. Tension (Brazilian) tests

The rock samples are 5.06 cm in diameter and 5.06 cm in length. They were subjected to the Brazilian tests. A single fracture was developed. The four loading rates are applied: 0.05, 0.1, 0.2 and 0.3 kN/s. Two examples of fracture surfaces developed under three different loading rates are shown in Fig. 1. Table 1 summarizes the petrological and petropyhsical properties of the samples. Effective porosity values were obtained from the laboratory measurements by the saturation method. Average grain sizes were determined through visual inspection of thin sections. The average grain sizes were also verified from the published data for different rock types [16]. Each sample was subjected to four different loading rates except sample L. Only three loading rates, 0.05, 0.1 and 0.2 kN/s, were applied for this sample.

3. Data acquisition

To map the surface roughness of fractures, a computer controlled mechanical device was used. The details of the device can be found in [17]. Measurements [18–20] for different rock fracture surfaces have been made. 32×32 data points, 1 mm apart, were acquired through this system. Accuracy of the data acquisition scheme [17] and fractal measurements [19] can be found in the relevant references. 3D views of two fracture surfaces are illustrated in Fig. 2.

4. Determination of fractal dimension

Numerous methods have been introduced for the fractal analysis of fracture surfaces. The reliability of these methods still leaves much to be desired [21]. The fracture surface roughness was

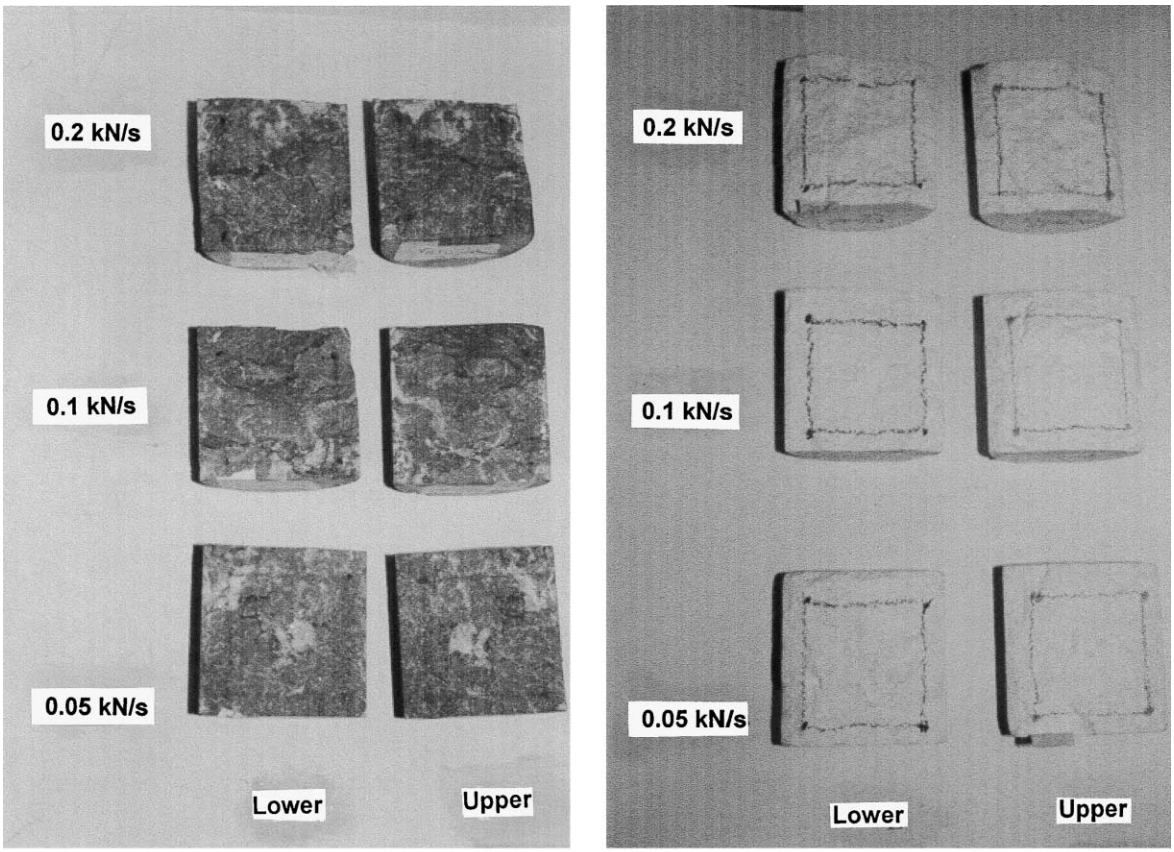

Fig. 1. (a) Photo of the fracture surfaces created under different tensional stresses (rock sample L). The diameter of the semi-cylindrical sample is 2 in. (b) Photo of the fracture surfaces created under different tensional stresses (rock sample K). The diameter of the semi-cylindrical sample is 2 in.

Table 1
Rock type used throughout the study and their petrophysical and pertrological properties

Rock no	Rock type		Effective porosity (%)	Average grain size (mm)	Thin section description
D	Diabase	Igneous	0.26	2	Coarse crystal, weathered, quartz filling micro-fractures. No void space
E	Limestone	Sedimentary	1	0.25	Porous, micritic, limestone (travertine). Secondary calcite crystallization. Pore sizes between 0.2 and 4 mm. Low Fe-oxide. High void space
F	Sandstone	Sedimentary	1.65	0.6	Rich for quartz. Contains feldspar and mica
G	Andesite	Igneous	4.5	0.002	Rich for pyroxene minerals. Void space is observed
J	Granite	Igneous	0.6	2	Rich for amphibole and biotite. Low weathering
K	Limestone	Sedimentary	7.2	0.5	Cemented sandy limestone. High weathering. Contains mica and amphibole. Contains pores
L	Recrystallized limestone	Metamorphic	0.05	2	Cemented, red–dark-brown colored recrystallized limestone. Contains Fe-oxide. Micritic texture

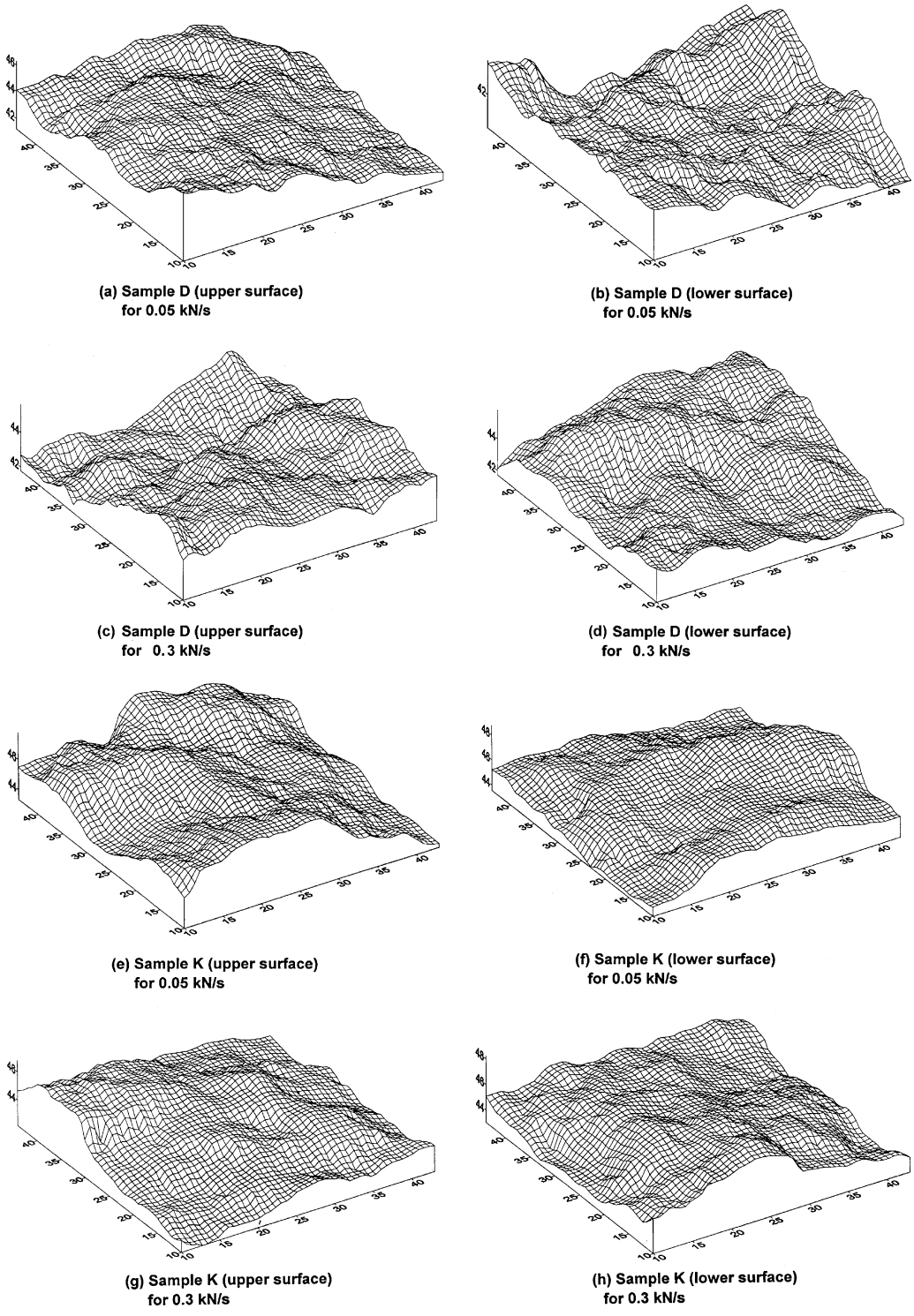

Fig. 2. Two examples of fracture surfaces. 32×32 surface data acquired by a fully automated surface scanning device.

observed as self-affine fractal [18,22–25]. The 1D power spectral and variogram analyses have been used in [2,3,24]. Recently, 2D date sets have been applied [18] for different methods to measure the fractal dimension of natural fracture surfaces. The fractal profiles obtained by the VA do not approach the fractal dimension of 2D data set obtained by power spectral analysis if the value is simply added to one. Provided in [26,27] are also an extensive comparison analysis of the methods used to measure the fractal dimension of fracture surfaces. These comparative studies conclude that the VA can be easily applied to measure the fractal dimension of surface profiles and yields consistent results with other techniques for 1D data set.

4.1. Power spectral density analysis

Power spectral density (PSD) analysis is commonly applied to calculate the fractal dimension of both fracture profiles and surfaces. The fractal dimension of a two-dimensional set can be calculated from the slope of a log–log plot of power, $S(k)$ vs. wavenumber, k. The relationship between $S(k)$ and k is given by

$$S(k) \propto k^{-\beta} \tag{1}$$

where β is the slope of the log–log plot. The fractal dimension D is related to the slope β of log–log plot as [28]:

$$D = (8 + \beta)/2 \tag{2}$$

The PSD of a topologically two-dimensional fracture surface can be calculated with two-dimensional Fourier transform. Two-dimensional Fourier transform of a given complex function $z(p_1, p_2)$ is calculated over the grid by the equation

$$z(n_1, n_2) = \sum_{p_1=0}^{N_1-1} \sum_{p_2=0}^{N_2-1} z(p_1, p_2) \mathrm{e}^{-\mathrm{i}2\pi\left(\frac{p_1 n_1}{N_1} + \frac{p_2 n_2}{N_2}\right)} \tag{3}$$

where N_1 and N_2 refer to sample data along x and y direction respectively, p_1 and p_2 are index values used in consecutive data spatial domain along the x and y direction, respectively, where $0 \leqslant p_1 \leqslant N_1 - 1$ and $0 \leqslant p_2 \leqslant N_2 - 1$. Here, n_1 and n_2 are index values used in wavenumber sampling along x and y direction respectively, such that $0 \leqslant n_1 \leqslant N_1 - 1$ and $0 \leqslant n_2 \leqslant N_2 - 1$.

With this equation, the two-dimensional data, can be transformed to the wavenumber k space. After the transformation, the PSD analysis can be calculated as

$$|z(n_1, n_2)|^2 = \mathrm{R}^2 z(n_1, n_2) + \mathrm{I}^2 z(n_1, n_2) \tag{4}$$

where $\mathrm{R}z(n_1, n_2)$ and $\mathrm{I}z(n_1, n_2)$ are the real and imaginary part of the Fourier transform, respectively.

4.2. Variogram analysis

The variogram is defined as the mean squared increment of points

$$\gamma(h) = \frac{1}{2n}[V(x_i) - V(x_{i+h})]^2 \tag{5}$$

where $\gamma(h)$ is the semi-variogram and n is the number of pairs at a lag distance and h and $V(x_i)$ and $V(x_{i+h})$ are the sample values at location x_i and x_{i+h}.

The variogram that has been used for spatial analysis in geostatistics can also be used to estimate the fractal dimension of natural surfaces. If the variogram $\gamma(h)$ is plotted against lag distance, h on a log–log paper, the slope yields the Hurst exponent, H according to

$$\gamma(h) = \gamma_0 h^{2H} \tag{6}$$

Here, H is related to the fractal dimension by $D = 2 - H$ while H is the half of the slope of lag distance. The variogram involves plotting h vs. $\gamma(h)$.

5. Analysis of the results

The analysis was done in two different ways. First, the 2D set as a whole was evaluated. Next, 1D sets were analyzed individually to account for the anisotropic nature of the fractal characteristics of the surface data. Both upper and lower surfaces of the fracture were considered. PSD analysis was performed only for the fractal dimension of the surface. VA was applied for the fractal dimension and intercept value (γ_0 in Eq. (6)).

5.1. Power spectral density analysis

The fractal dimensions of fracture surfaces for seven rocks were calculated using the PSD method. The values obtained by this method are expected to be between 2 and 3 if the fracture surface represents fractal characteristic. All the surfaces with a few exceptions gave values between 2 and 3 as seen in Fig. 3. These exceptions are slightly lower than 2. The fractal dimension values are less than 2.5 with only one exception. No typical trend or behavior is observed for all the rock samples. There is a noticeable difference between the fractal dimensions of upper and lower parts of the samples E, F, G, J and K. Obviously, sample type plays a role on the fracture characteristics. The inconsistencies between the fractal dimensions of upper and lower surfaces are related to petrological–mineralogical and petrophysical properties of the rock samples. This will also control the surface roughness of fracture. Note that samples E and K are limestones, sample F is sandstone, sample G is andesite and sample J is granite, Table 1. Limestone, sandstone and ande-

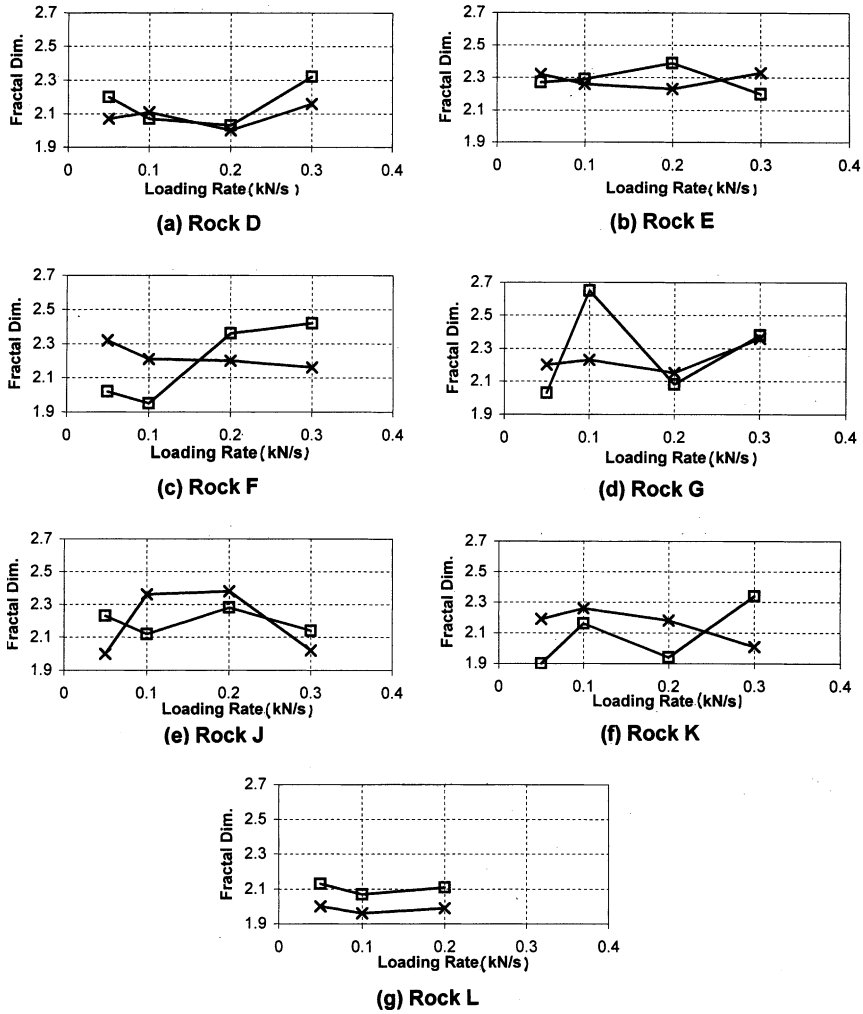

Fig. 3. Fractal dimension of the upper and lower surfaces against the loading rate for the rock types given in Table 1. Method applied: PSD. × Upper surface; □ lower surface.

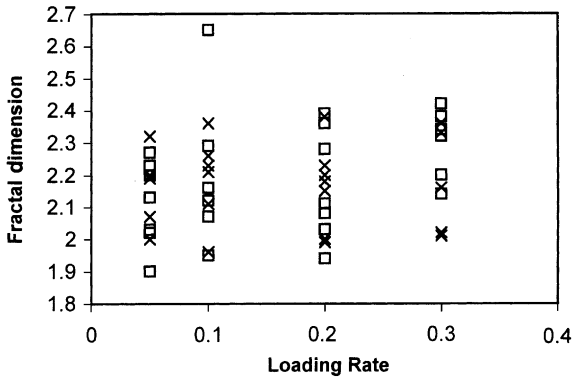

Fig. 4. Change of surface fractal dimension obtained by PSD with the loading rate for all samples given in Fig. 3. × Upper surface; □ lower surface.

site samples contain pore space. Thin section views revealed that the grain sizes are between 0.25 and 0.6 mm for both sandstone and limestone samples (Table 1). The exceptional case was sample J (granite). The porosity of this sample was very low but the grain size (2 mm) was greater than the other samples.

In order to obtain a general insight into the relationship between the fractal dimension and loading rate, all the data shown in Fig. 3 were plotted together in Fig. 4. No quantitative correlation has been withdrawn due to scattered nature of the data but a general trend can be observed in this graph. As seen, the fractal dimension increased with increasing loading rate.

5.2. Variogram analysis

The fractal dimensions of 32 profiles from the vertical and horizontal directions were calculated using a maximum lag distance h of six. Horizontal and vertical profiles correspond to the parallel direction of loading and vertical to the orthogonal direction of loading. The scanning directions are shown in Fig. 5 schematically. Fracture surfaces were evaluated using fractal dimension and intercept values. The arithmetic means of the fractal dimension and intercept values (γ_0 in Eq. (6)) of 32 profiles were taken as the fractal dimension and intercept values for the whole surface.

5.2.1. Average fractal dimension

The average values were calculated for 32 fractal profiles in the vertical or horizontal direction. The change of these fractal dimensions with the loading rate for both vertical and horizontal profiles are shown in Fig. 6. All the fractal values fell within the range between 1 and 2 implying that they all represent fractal feature. The fractal dimensions of upper and lower surfaces are in agreement for all the cases except sample K. This is in accordance with the PSD fractal dimensions, Fig. 3. But samples E, F, G and J also yield non-matching fractal dimensions of the upper and lower surfaces for PSD measurements. Note that sample K with medium size grain has the highest porosity value. Sample G and F have the second

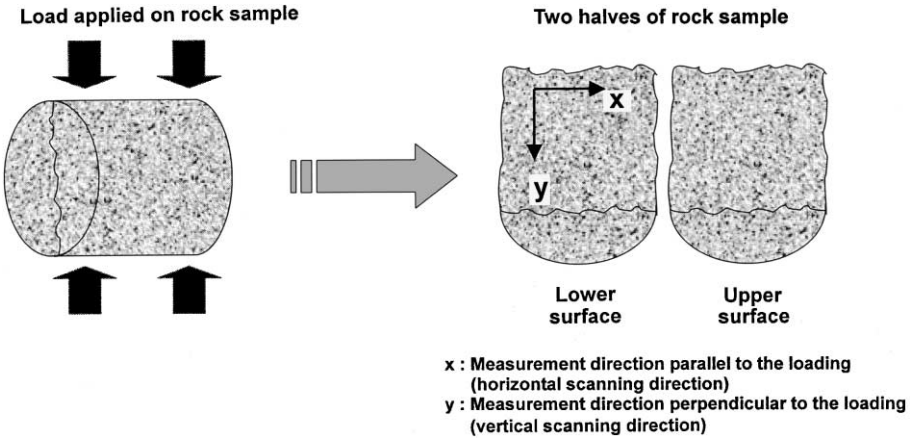

Fig. 5. Creation of fracture surfaces by the Brazilian test and the scanning directions to map the surface roughness.

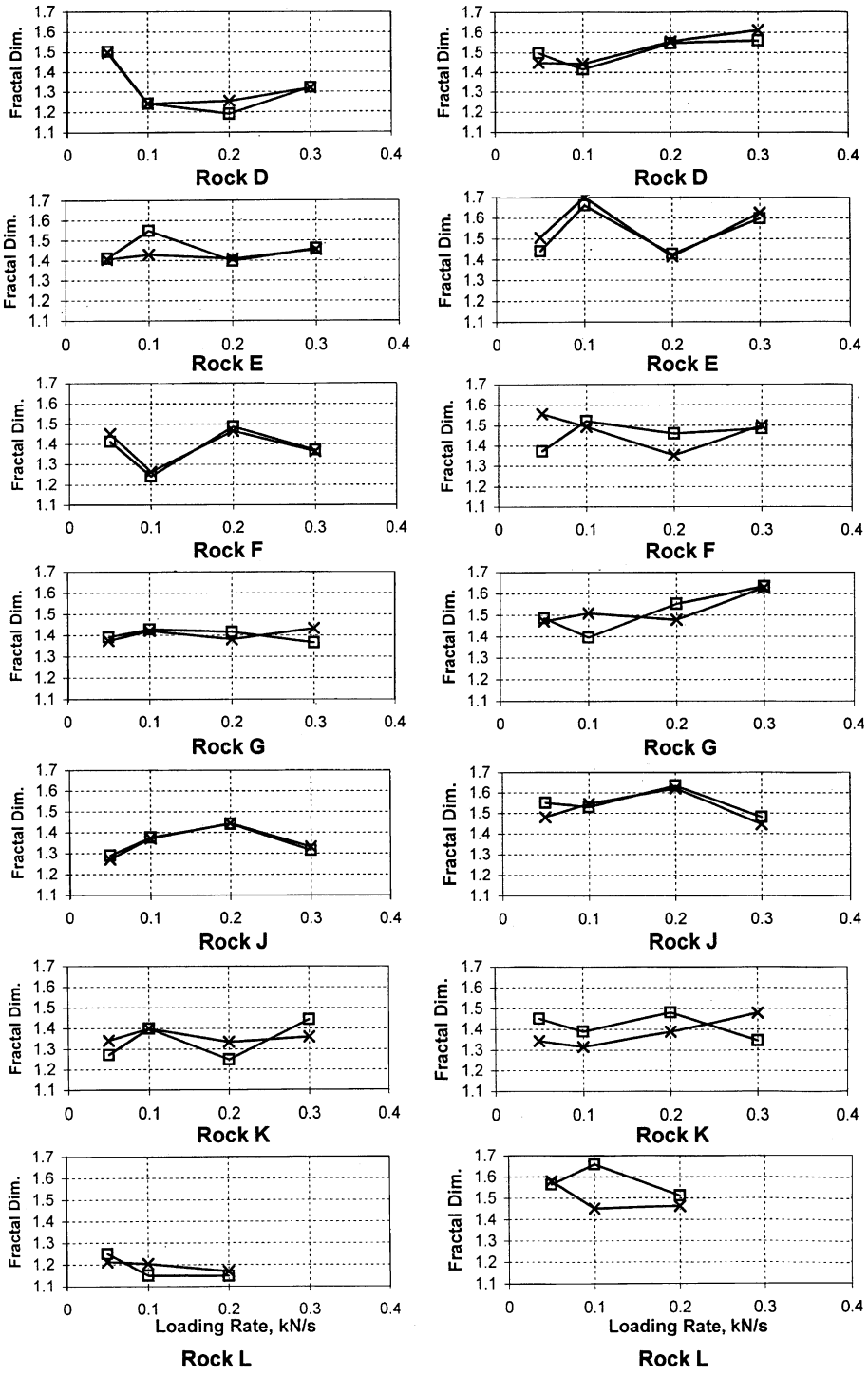

Fig. 6. Average fractal dimension values against the loading rate for both vertical (left) and horizontal (right) profiles for the rock types given in Table 1. Method applied: VA. × Upper surface; □ lower surface.

and third highest porosity among the seven samples, that are 4.5 and 1.65, respectively. In fact, sample G and F showed a notable difference between the fractal dimensions of upper and lower surfaces in the horizontal direction. It should also be emphasized that the difference between the upper and lower surfaces was more pronounced for the horizontal direction profiles than the vertical ones. These observations divulge that porosity and grain size can be correlated by variogram fractal dimensions.

It was observed that the trend of fractal dimension change with the loading rate was quite similar to the PSD analysis. The difference between the upper and lower surface fractal dimensions were much smaller than those of PSD fractal dimensions. Some exceptional cases exist. For sample J, PSD fractal dimensions for the vertical and horizontal lines were quite far apart, Fig. 3. In contrast, both methods revealed a similar behavior for sample K for the difference between upper and lower fractal dimensions. Interestingly, the trend of fractal dimension change with the loading rate is very similar for both PSD and VA for sample K. Note also that similar trends were observed for the vertical and horizontal profiles even though the fractal dimensions for the latter are higher in all cases for both upper and lower surfaces. Observed in [10] are the opposite when porous sandstone samples are used. The fractal dimension in loading direction (horizontal direction) is lower than those in the direction perpendicular to the loading. Further discussion on this will be made later.

Fractal dimension describes the irregularity of the surface roughness, i.e. higher fractal dimension corresponds to rougher fracture surface [11]. Sample D exhibits the lowest fractal dimension for higher loading rates in the vertical direction. This implies that the surface is smoother than all others. In vertical direction, other samples represent fractal dimension values between 1.2 and 1.4. In horizontal direction, however, samples D and E have the highest fractal dimensions. The lowest fractal dimension in this direction was obtained for sample K. Note that sample D and K represent the lowest and highest porosities, respectively. At first sight, it may be concluded that the horizontal fractal dimensions becomes higher as the porosity decreases. Two limestone samples (sample E and K) showed different behavior. This can be attributed to the grain size and porosity of the sample. Sample E presents calcite recrystallization and this might be the reason for a much lower porosity than the other limestone sample K. For all the rock samples, fractal dimension in the horizontal direction is higher. This means that the surface in this direction is rougher.

5.2.2. Average intercept value

Recent studies showed that the fractal dimension is insufficient to quantify the surface roughness [9,11,13]. Different fractal properties were used in different studies for characterizing surface roughness. The use of intercept value in Eq. (6) for correlation has been proposed in [10,11]. These studies show that the intercept is an indicator of asperities. The steeper the asperity, the greater is the y-intercept [11].

Analyzed also is the change of intercept with the loading rate, Fig. 7. The trend is similar to the fractal dimension change against the loading rate but no typical correlation was observed. The difference between the upper and lower surfaces is trivial for all the cases except for samples G and K. This difference for the fractal dimension change with the loading rate is in the same manner as in Fig. 6. The reason of this change is again the high porosity of the two samples.

All the data given in Figs. 6 and 7 for the PSD analysis were plotted for both the vertical and horizontal lines. The plots are shown in Fig. 8. The aim is to observe the general trend of the mineralogical and petrophysical properties of the rock. A second degree polynomial curve was fitted. The intercept value exhibits a decreasing trend with the loading rate for both vertical and horizontal profiles, Fig. 8(a) and (b). The fractal dimension changes with the loading rate, however, was not significant, Fig. 8(c) and (d). It is almost a zero-slope straight line for vertical profiles. The change is more pronounced for horizontal profiles. There exists minimum and maximum values for upper and lower surfaces, respectively, Fig. 8(d). These points coincide with the loading rate values between 0.15 and 0.2 kN/s.

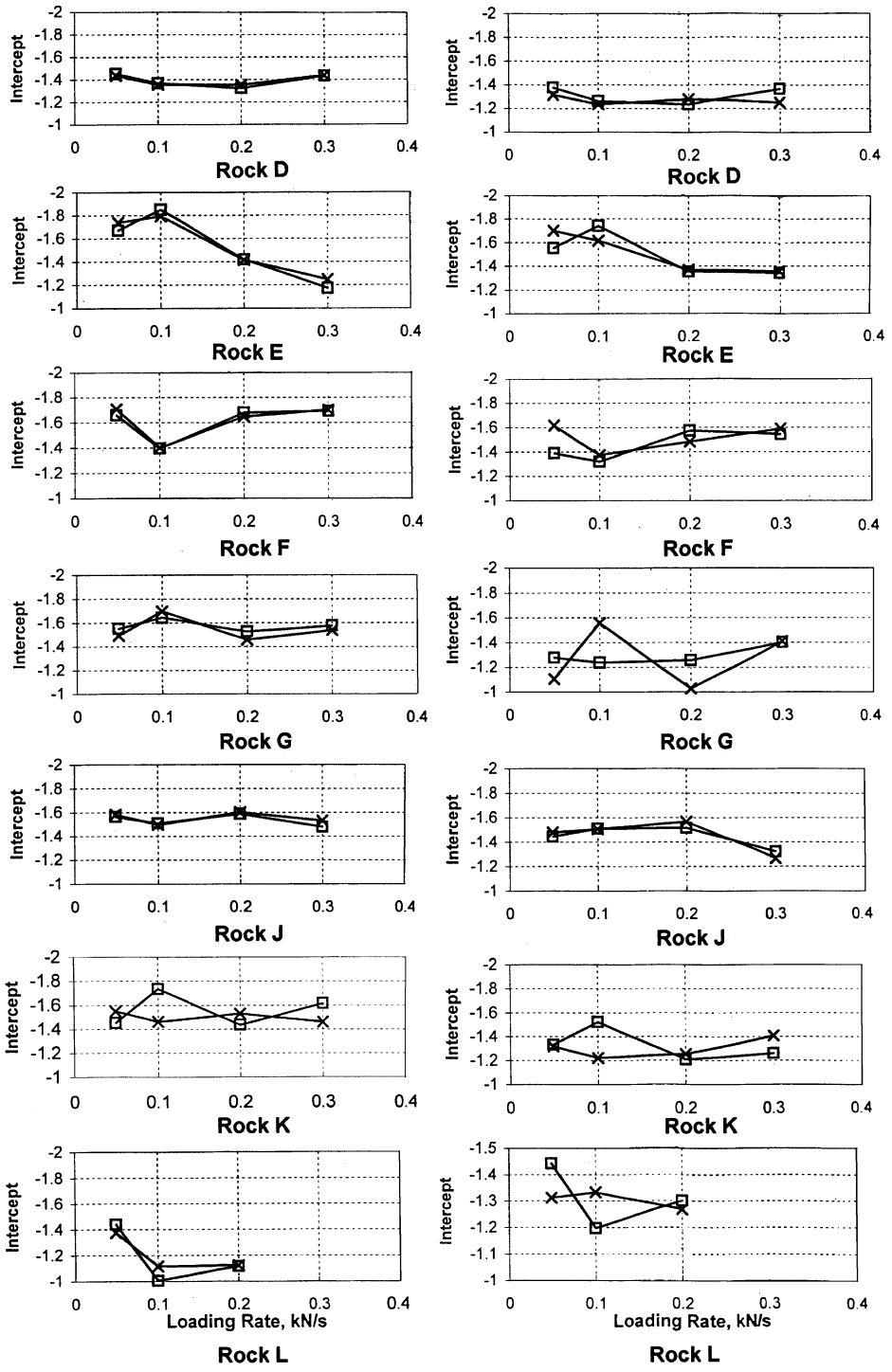

Fig. 7. Average intercept values (γ_0 in Eq. (6)) against the loading rate for both vertical (left) and horizontal (right) profiles for the rock types given in Table 1. Method applied: VA. × Upper surface; □ lower surface.

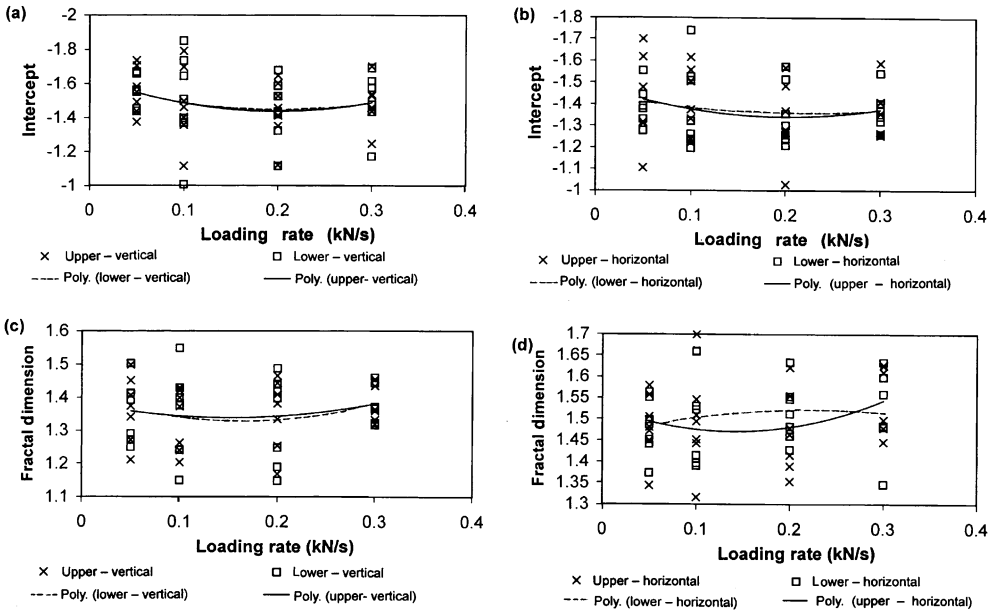

Fig. 8. Change of intercept and fractal dimension obtained by VA with the loading rate for all samples given in Figs. 6 and 7.

5.2.3. Evaluation of the fractal properties of profiles individually

The fractal dimensions and intercepts obtained through VA were examined individually. Evaluated in [10,12] are the fractal dimensions of individual profiles obtained by the VA and divider method. Different fractal dimensions are obtained for all profiles individually. The fractal dimensions are found to vary with the direction for both tensile and shear fracture. The fractal dimension for profiles parallel to the loading directions, that corresponds to the horizontal profiles (see Fig. 3) are greater than those in the perpendicular direction [12]. The opposite was observed in [10] for variogram fractal dimensions. In the present case, the horizontal dimensions were higher than the vertical ones. This is in agreement with the divider measurements [12] but not with the variogram dimensions of porous sandstone surfaces [10].

Four extreme cases are given in Figs. 9 and 10 for the slope and intercept values of the profiles, respectively. The slope is related to the fractal dimension for $D = 2 - H$. Rock samples D and F represent the cases for which the slope and intercept values are considered to be in good agreement for vertical and horizontal profiles. Samples J and K, however, exhibit significant difference in the slopes and intercepts.

The differences between the intercept, slope and fractal dimension of the upper and lower surface profiles were also analyzed. The differences were obtained by subtracting the lower surface values from the upper surface. For sample G, all three loading rates yield significant difference in the slopes. This is more significant for the lower loading rates of 0.05, 0.1 and 0.2 kN/s. For samples E and F, the difference is notable for the loading rate of 0.05 kN/s. The same can be said for the loading rate of 0.3 kN/s for sample K. The differences are not significant for the sample D and J.

Individual fractal dimensions of profiles do not reveal any information because they differ from adjacent one. But the average value may have some implications regarding to the surface roughness, Fig. 6. Typically, lowest difference between the upper and lower surfaces were observed in the middle portion of the samples in the vertical direction (orthogonal to loading). This was not observed for the horizontal profiles. This local change in the fractal dimension (or roughness) is

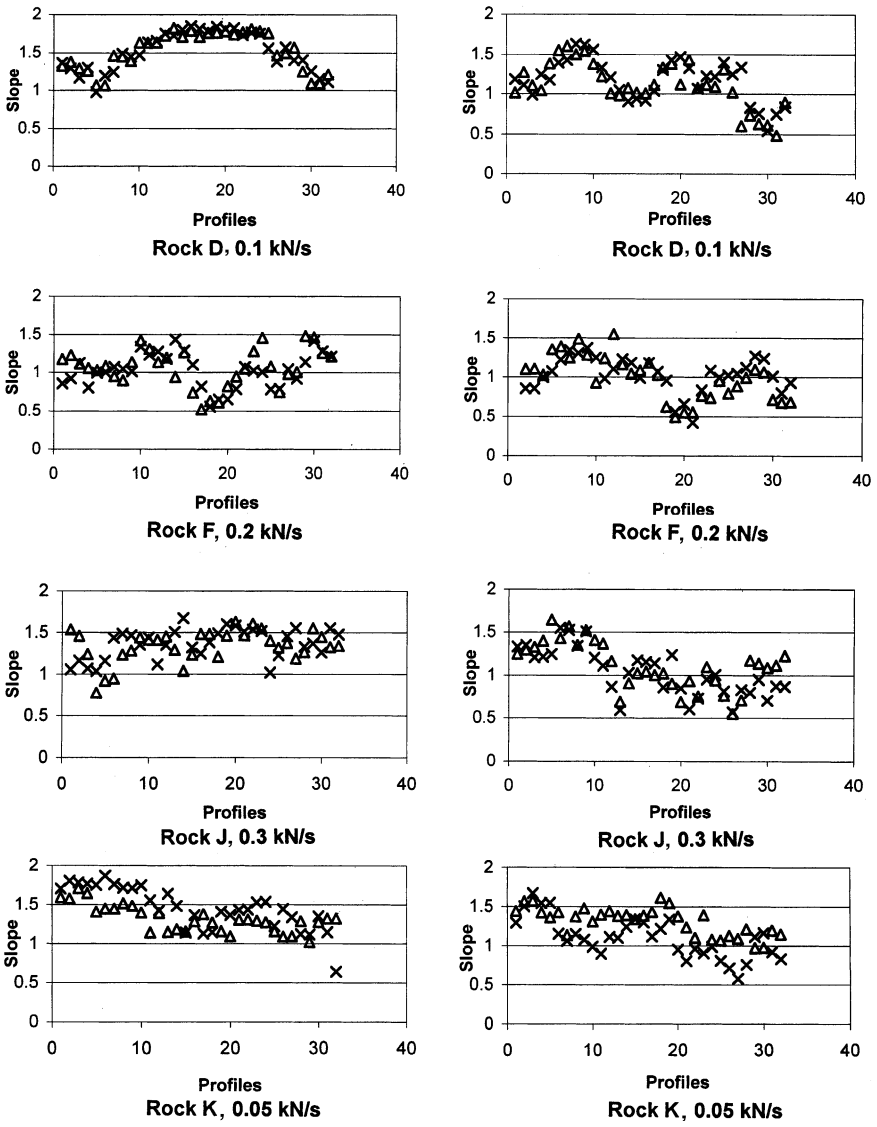

Fig. 9. Slope values of the profiles of upper and lower surfaces in vertical (left) and horizontal (right) directions for samples D, F, J and K. △ Upper surface; × lower surface.

expected to be related to the stress condition causing fractures.

5.3. Relationship between grain size/porosity and fractal dimension

Analysis was carried out for relating porosity–grain size to the fractal dimension of surface. PSD fractal dimensions showed a decreasing trend with the grain size, Fig. 11(a). No correlation with the porosity, Fig. 11(b) was obtained. VA fractal dimensions yield a similar trend with the grain size, Fig. 12(a). They also gave a correlation with the porosity, Fig. 12(b). It was found that the peak fractal dimension is obtained for the porosity value around 1%, Fig. 12(b). This is valid for all four loading rates; as it can be seen from Fig. 13(b). In short, porosity is more sensitive to the

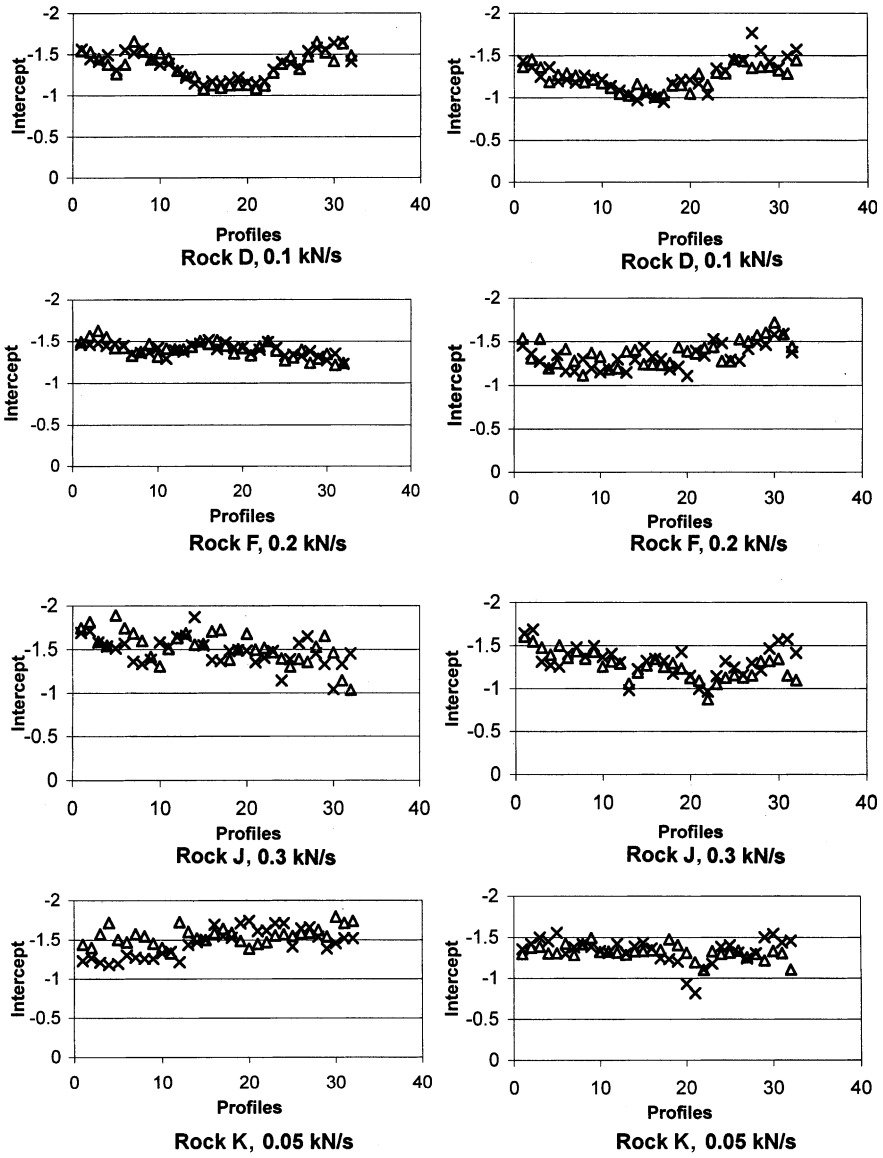

Fig. 10. Intercept values of the profiles of upper and lower surfaces in vertical (left) and horizontal (right) directions. △ Upper surface; × lower surface.

surface roughness than the grain size. The grain size showed no correlation. The curve is almost a straight line with zero slope for the variogram fractal dimensions of vertical profiles, Fig. 13(a). The only point worthwhile emphasizing is that more scattered fractal dimension values were obtained for the higher grain sizes. The fractal dimension for the smaller grain sizes (<0.5 mm) were much closer to each other for different loading rates.

To summarize the observations:

- No trend was observed for the change of fractal dimension with loading rate when the samples were analyzed individually. When all the samples were considered, however, it was found that

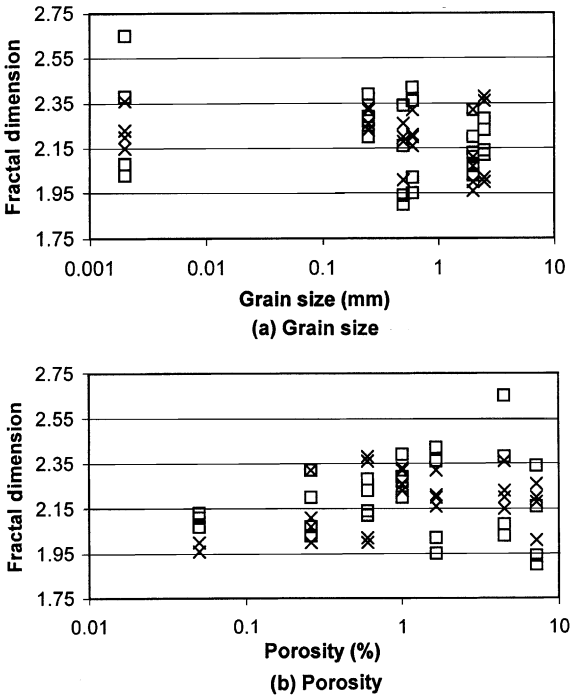

Fig. 11. Relationship between the fractal dimension and (a) grain size and (b) porosity for all samples given in Table 1. Method: PSD analysis. × Upper surface; □ lower surface.

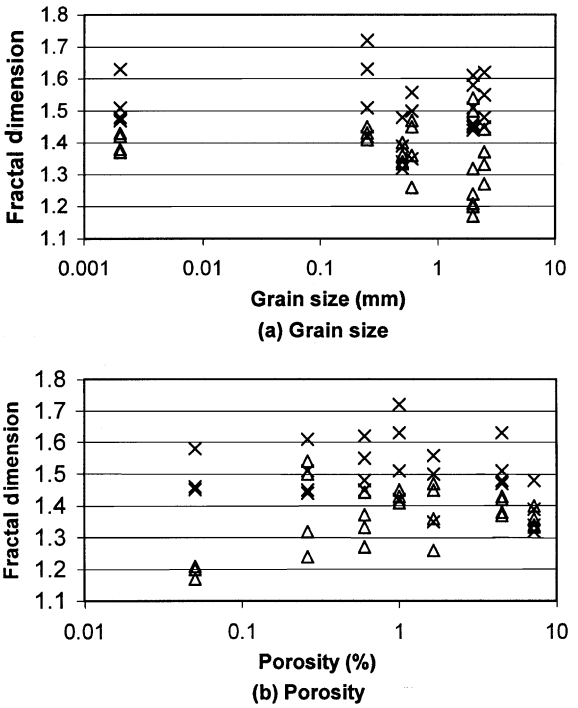

Fig. 12. Relationship between the fractal dimension and (a) grain size and (b) porosity for all samples given in Table 1 for horizontal and vertical profiles (upper surfaces only). Method: VA. × Horizontal profiles; △ vertical profiles.

there exists a certain trend between the loading rate and fractal dimension.

- Profiles parallel to the loading yield higher fractal dimensions than those perpendicular to the loading.
- The difference between the upper and lower samples was attributed to the porosity of the sample. Higher porosity resulted in a higher difference between the fractal dimension of the two surfaces. Thus, more tortuosity is expected with increasing porosity.

6. Conclusions and remarks

This research questions whether the fractal properties of fracture surfaces could be used to explain rock property and fracture behavior. To this end, the PSD and VA were applied to calculate the fractal dimensions of fracture surfaces. The Brazilian test was used to create fracture surfaces. No typical behavior was observed to define a relationship between the fractal dimension and loading rate when the evaluation is made for each rock sample individually. A trend seems to prevail when the all samples were plotted together. PSD dimension and intercept value from VA showed a decreasing trend of fractal dimension with the loading rate. For the samples that contain more pores such as limestone and sandstone, and granite with no pores bigger than grain size, upper and lower fracture surfaces exhibited difference in fractal dimension. This difference is more pronounced for the profiles parallel to the loading.

PSD fractal dimensions showed a decreasing trend with the grain size but no correlation with the porosity. VA fractal dimensions exhibited a similar trend with the grain size but they also presented a correlation with the porosity. It was found that a peak fractal dimension value exists; it corresponds to porosity value around 1%. This

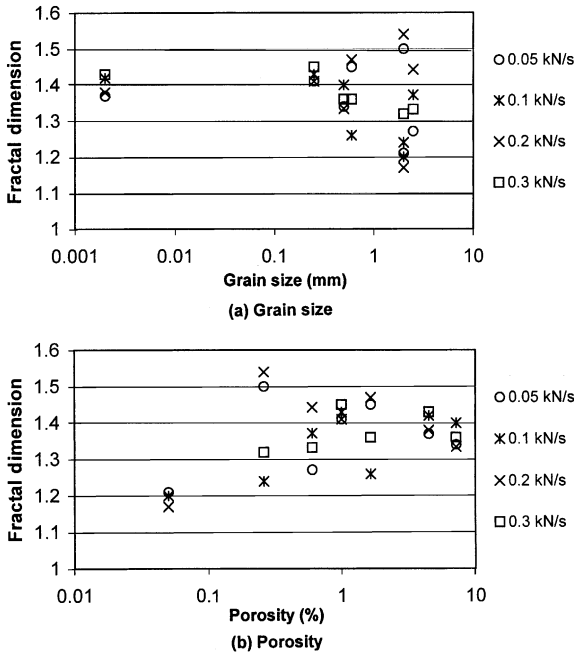

Fig. 13. Relationship between the fractal dimension and (a) grain size and (b) porosity for all samples given in Table 1 for different loading rates (upper surfaces and vertical profiles only). Method: VA.

was valid for all four loading rates. Porosity was observed more sensitive to the surface roughness than the grain size.

Acknowledgements

Thanks are due to S. Avsar for his help during the Brazilian tests. Appreciation is also extended to C. Comlekci for his advice and help in designing the surface roughness measurement device and software.

References

[1] B.B. Mandelbrot, D.E. Passoja, A.J. Paullay, Fractal character of fracture surfaces of metals, Nature 308 (1984) 721–722.
[2] S.R. Brown, S.H. Scholz, Broad bandwidth study of the topography of natural rock surfaces, J. Geophys. Res. 90 (14) (1985) 12575–12582.
[3] S.R. Brown, A note on the description of surface roughness using fractal dimension, Geophys. Res. Lett. 14 (11) (1987) 1095–1098.
[4] J. Schmittbuhl, S. Roux, Y. Berthaud, Development of roughness in crack propagation, Europhys. Lett. 28 (8) (1994) 585–590.
[5] Y.H. Lee, J.R. Carr, D.J. Barr, C.J. Haas, The fractal dimension as a measure of the roughness of rock discontinuity profiles, Int. J. Rock Mech. Min. Sci. Geomech. Abstr. 27 (6) (1990) 453–464.
[6] N. Wakabayashi, I. Fukushige, Experimental study on the relation between fractal dimension and shear strength, in: L.R. Myer, N.G.W. Cook, R.F. Goodman, C.F. Tsang (Eds.), Fractured and Joint Rock Masses, Balkema, Rotterdam, 1995, pp. 119–124.
[7] Z.Y. Yang, G.L. Chen, Application of the self-affinity concept to the scale effect of joint roughness, Rock Mech. Rock Eng. 32 (3) (1999) 221–229.
[8] S.D. Lee, C.I. Lee, Y. Park, Characterization of joint profiles and their roughness parameters, Int. J. Rock Mech. Min. Sci. 34 (3/4) (1997) 709.
[9] P.H.S.W. Kulatilake, G. Shou, T.H. Huang, R.M. Morgan, New peak shear strength criteria for anisotropic rock joints, Int. J. Rock Mech. Min. Sci. Geomech. Abstr. 32 (7) (1995) 673–697.
[10] H. Xie, J. Wang, W.H. Xie, Fractal effects of surface roughness on the mechanical behavior of rock joints, Chaos Soliton. Fract. 8 (2) (1997) 221–252.
[11] M.A. Kwasniewski, J.A. Wang, Surface roughness evolution and mechanical behavior of rock joints under shear, Int. J. Rock Mech. Min. Sci. 34 (3/4) (1997) 709.
[12] H. Xie, J. Wang, M.A. Kwasniewski, Multifractal characterization of rock fracture surfaces, Int. J. Rock Mech. Min. Sci. 36 (1999) 19–27.
[13] T. Belem, F. Homand-Etienne, M. Souley, Fractal analysis of shear joint roughness, Int. J. Rock Mech. Min. Sci. 34 (3/4) (1997) 395.
[14] D.A. Lange, H.M. Jennings, S.P. Shah, Relationship between fracture surface roughness and fracture behavior of cement paste and mortar, J. Am. Ceram. Soc. 76 (3) (1993) 589–597.
[15] Z.X. Zhang, J. Yu, S.Q. Kou, P.-A. Lindqvist, On study of influences of loading rate on fractal dimensions of fracture surfaces in gabbro, Rock Mech. Rock Eng. 34 (3) (2001) 235–242.
[16] R.B. Johnson, J.V. DeGraff, Principles of Engineering Geology, John Wiley & Sons, 1988.
[17] K. Develi, T. Babadagli, C. Comlekci, A new computer controlled surface scanning device for measurement of fracture surface roughness, Comput. Geosci. 27 (3) (2001) 265–277.
[18] K. Develi, T. Babadagli, Quantification of natural fracture surfaces using fractal geometry, Math. Geol. 30 (8) (1998) 971–996.
[19] T. Babadagli, K. Develi, Fractal analysis of natural and synthetic fracture surfaces of geothermal reservoir rocks, in: Proceedings 2000 World Geothermal Congress, Kyushu-Tohoku, Japan, May 28–June 10, 2000, pp. 2515–2520.

[20] T. Babadagli, K. Develi, On the application of methods used to calculate fractal dimension of fracture surfaces, Fractals 9 (1) (2001) 105–128.
[21] S.M. Miller, P.C. McWilliams, J.C. Kerkering, Ambiguities in estimating fractal dimensions of rock fracture surfaces, in: W. Hustrulid, G.A. Johnson (Eds.), Rock Mechanics Contributions and Challenges, Balkema, Rotterdam, 1990, pp. 471–478.
[22] B.B. Mandelbrot, Self-affine fractals and fractal dimension, Physica Scripta 32 (1985) 257–260.
[23] M. Sakellariou, B.B. Nakos, C. Mitsakaki, On the fractal character of rock surfaces, Int. J. Rock Mech. Min. Sci. Geomech. Abstr. 28 (6) (1991) 527–533.
[24] S.L. Huang, S.M. Oelfke, R.C. Speck, Applicability of fractal characterization and modeling to rock joint profiles, Int. J. Rock Mech. Min. Sci. Geomech. Abstr. 29 (2) (1992) 89–98.
[25] A. Den Outer, J.F. Kaashoek, H.R.G.K. Hack, Difficulties with using continuous fractal theory for discontinuity surfaces, Int. J. Rock Mech. Min. Sci. Geomech. Abstr. 32 (1) (1995) 3–9.
[26] A.R. Mehrabi, H. Rassamdana, M. Sahimi, Characterization of long-range correlations in complex distributions and profiles, Phys. Rev. E 56 (1) (1997) 712–722.
[27] J. Schmittbuhl, J.-P. Vilotte, S. Roux, Reliability of self-affine measurements, Phys. Rev. E 51 (1) (1995) 131–147.
[28] P.R. La Pointe, C.C. Barton, Creating reservoir simulations, in: C.C. Barton, P.R. La Pointe (Eds.), Fractals in Petroleum Geology and Earth Processes, Plenum Press, New York, 1995, pp. 267–268.